International Journal of Heat and Mass Transfer 53 (2010) 1673–1681

Contents lists available at ScienceDirect

International Journal of Heat and Mass Transfer

journal homepage: www.elsevier.com/locate/ijhmt

Preparation and pool boiling characteristics of copper nanofluids over a flat plate heater

R. Kathiravan [a], Ravi Kumar [a,*], Akhilesh Gupta [a], Ramesh Chandra [b]

[a] Department of Mechanical and Industrial Engineering, Indian Institute of Technology Roorkee, Roorkee 247 667, India
[b] Institute Instrumentation Centre, Indian Institute of Technology Roorkee, Roorkee 247 667, India

ARTICLE INFO

Article history:
Received 2 January 2009
Received in revised form 14 July 2009
Accepted 10 November 2009
Available online 6 February 2010

Keywords:
Nanofluids
Copper nanoparticles
Critical heat flux
Sputtering
Boiling

ABSTRACT

The copper nanoparticles of average size of 10 nm have been prepared by the sputtering method and characterized through atomic force microscopy (AFM), X-ray diffraction (XRD) and transmission electron microscopy (TEM). The pool boiling heat transfer characteristics of 0.25%, 0.5% and 1.0% by weight concentrations of copper nanoparticles has been studied. Different copper based nanofluids were prepared in both, distilled water and distilled water with 9.0 wt% of sodium lauryl sulphate anionic surfactant (SDS). The pool boiling heat transfer data were acquired for the boiling of nanofluids over a 30 mm square and 0.44 mm thick stainless steel plate heater. The experimental results show that for the critical heat flux of pure water is 80% higher than that of water–surfactant fluid. Also, it was found that the critical heat flux for 0.25%, 0.5% and 1.0% concentrations of copper nanoparticles in copper–water nanofluids are 25%, 40% and 48% higher than that of pure water. But in the case of copper–water with surfactant nanofluids comparing with pure water, the CHF decreases to 75%, 68%, and 62% for respective concentrations of copper nanoparticles. The heat transfer coefficient decreases with increase of nanoparticles concentration in both water–copper and water–copper with surfactant nanofluids.

1. Introduction

For decades extensive investigations have been carried out to study the pool boiling of various fluids like water, refrigerant, etc. Recently the pool boiling studies have drawn attention of scientists and engineers owing to growing demand of high energy dissipation in electronic equipment and computing machines. Earlier, Rohsenow [1] and Cornwell and Houston [2] reported the boiling heat transfer coefficient of water over various heating surfaces, through mathematical approach based in the principles of physics and by conducting experiments as well. Later, Pioro [3] experimentally determined the heat transfer of water, ethanol, R-113 and R-11 under nucleate boiling on copper, aluminum brass and stainless steel plates. The effect of the thermo-physical properties of a boiling surface "conjugate effect" on the heat transfer coefficient during pool boiling resulted in the increase of heat transfer coefficient with decreasing saturation pressure, below the atmospheric pressure. Choi [4] found that the particles of the size of nanometer, suspended with conventional fluids, enhance the heat transfer. However, the sedimentation of particles was observed, which was rectified by Xuan et al. [5,6] by adding small amount of surfactant, like laurate salt, in water. They found that the erosion and pressure drop during the flow was significantly reduced due to powder form of these nano-size particles and the thermal conductivity of the base fluid was greatly enhanced. Lee et al. [7] found the enhancement of thermal conductivity in a range of 7–30% when Al_2O_3 and CuO nanoparticles were suspended with water and ethylene glycol in 1–5% particle volume fraction. Eastman et al. [8] also revealed an increase of 40% convective heat transfers with 2.0% nanoparticle concentration. Nanofluids have also significant bearing on critical heat flux (CHF). Vassallo et al. [9] have reported the considerable increase of CHF using 0.5% water–SiO_2 nanofluids. On the other hand, You et al. [10] have also observed the significant CHF enhancement with water–Al_2O_3 nanofluids at concentrations as low as 0.0001%. The pool boiling of Al_2O_3 nanofluid by Das et al. [11,12] was experimentally investigated, and it was found that the addition of nanoparticles deteriorated the boiling performance with increase in particles size. Kim et al. [13,14] conducted the pool boiling experiments on pure water over a Nicrome wires coated by TiO_2 and Al_2O_3. The experimental results reveal that the CHF was increased in of the order of 148% for 0.001% and 200% at 0.1% nanoparticles concentration of TiO_2, respectively. Further increase in nanoparticle concentration did not increase the CHF. However, in the case of Al_2O_3 based nanofluids the enhancement in CHF is 176% for particle concentration of 0.1%. This was because of the fact that microstructure and topography of the heater surface was modified by the deposition of suspended nanoparticles during the pool

* Corresponding author. Tel.: +91 1332 285740; fax: +91 1332 285665.
E-mail address: ravikfme@iitr.ernet.in (R. Kumar).

0017-9310/$ - see front matter © 2010 Elsevier Ltd. All rights reserved.
doi:10.1016/j.ijheatmasstransfer.2010.01.022

Nomenclature

A	heated surface area (m^2)
B	full width at half of maximum intensity (FWHM) in radians
Cp	specific heat capacity ($J\,kg^{-1}\,K^{-1}$)
I	electric current (A)
Nu	Nusselt number, hk_fL^{-1}
P	Pressure (Pa)
Pr	Prandtl number
R_a	average roughness (μm)
R_q	root mean square roughness (μm)
R_{max}	maximum roughness (μm)
R_k	coefficient of kurtosis
R_z	orthogonal direction roughness (μm)
Re_b	boiling Reynolds number
V	voltage (V)
a	side (m)
g	acceleration due to gravity ($m\,s^{-2}$)
h	heat transfer coefficient ($W\,m^{-2}\,K^{-1}$)
h_{fg}	latent heat of vaporization ($J\,kg^{-1}\,K^{-1}$)
k	thermal conductivity ($W\,m^{-1}\,K^{-1}$)
q	heat flux ($W\,m^{-2}$)
$\dot{q}_g$	internal volumetric heat generation rate ($W\,m^{-3}$)
k_w	thermal conductivity ($W\,m^{-1}\,K^{-1}$)
t	size of the nanoparticle (nm)

Greek symbols

δ	thickness of the plate (m)
ρ	density ($kg\,m^{-3}$)
Φ	fraction (%)
θ	maximum angle of reflection at which maximum intensity (°)
σ	surface tension (Pa m)
μ	viscosity (Pa s)
λ	wavelength of X-ray target (for copper it is 1.54 Å)

Subscripts

b	boiling
c	critical
f	fluid
g	vapor
m	mass
r	ratio
v	volume
w	wall, plate

boiling. Bang et al. [15] also found CHF enhancement due to surface coating of the heater surface with nanoparticles.

A review of the literature shows that most of the experimental studies are related to enhancement of the thermal conductivity and CHF of nanofluids containing Al_2O_3. In a few of the studies nanoparticles of SiO_2 also have been used [9]. Further, most of the work was carried out over either small diameter wire [5,6,9,10,13,14,16] or tubes having diameter less than 20 mm [11,12] with the average size of the nanoparticles around 20–50 nm. The research results of these investigations are not unique. Therefore, in order to understand the general behavior of this new fluid medium i.e. nanofluid, it is imperative to investigate the boiling of other nanofluids as well. Therefore, an experimental investigation has been carried out to study the pool boiling of nanofluids of different concentration of copper nanoparticles having average size of 10 nm in water, over a flat plate heater of 30 mm square size.

2. Preparation and characterization of nanofluid

In order to prepare nanofluids for present investigation the nanoparticles were generated by the sputtering method. In this method, the impact of an atom or ion on the target surface produces sputtering of particles from the surface as a result of the momentum transfer. Unlike other vapor phase techniques there is no melting of the material. The copper nanoparticles were generated using high pressure dc-magnetron sputtering. The sputtering target was a 50 mm diameter and 5 mm thick pure copper disc. The system was equipped with an arrangement to cool the substrate by continuously supplying liquid Nitrogen. During sputtering process the temperature was close to 100 K and the pressure was 10 mTorr of Argon gas. Before deposition, the chamber was evacuated to a base pressure of 0.5 mTorr. The average size of the nanoparticles measured by using Scherrer's formula [17] was approximately equal to 10 nm and the value of '2θ' and 'B' were determined by the XRD spectra.

2.1. X- ray diffraction (XRD) spectra of copper nanoparticle

The XRD test of nanoparticles was carried out in the laboratory. It was found that the copper nanoparticles were almost oriented with Miller indices of [1 1 1]. The average size of the particle was determined by the following Scherrer's formula [17]:

$$t = \frac{0.9\lambda}{B\cos\theta} \tag{1}$$

The graph shown in Fig. 1 depicts the X-ray diffraction spectra of copper nanoparticles taking intensity as abscissa and '2θ' as ordinate. The atomic structure of the majority of particles lied on the miller indices of [1 1 1] and small number of particles on indices [2 0 0]. It was also observed that the copper nanoparticles remained in pure copper state.

2.2. Atomic force microscopy (AFM) examination

Nanoparticles were also characterized by AFM in semi-contact mode. Fig. 2(a) shows the distribution of copper nanoparticles over a glass substrate mounted inside the chamber during the sputtering process. It was found that 8–10 nanoparticles were agglomerated with in the measured size of 100 nm when examined by AFM.

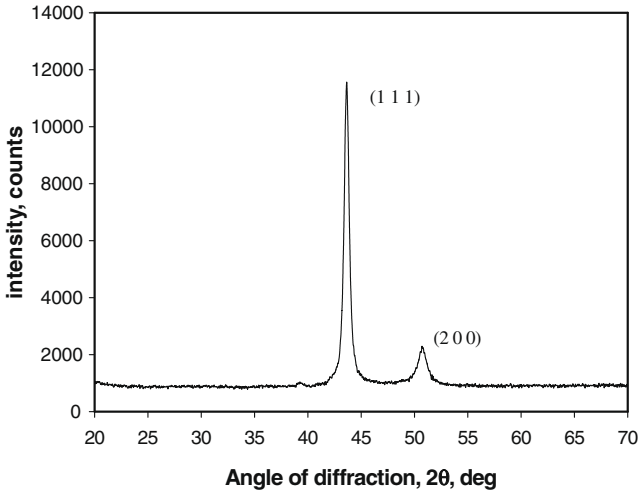

Fig. 1. Variation of intensity with angle of diffraction.

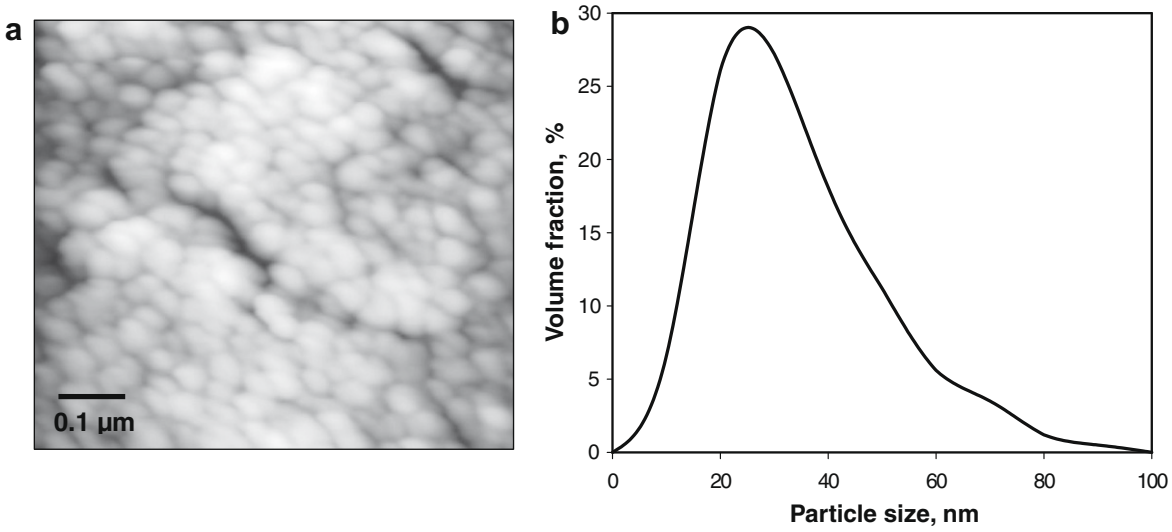

Fig. 2. (a) AFM picture of copper nanoparticles and (b) variation of particle size with percentage volume.

The [1 1 1] orientation of copper nanoparticles shows that the particles were of pure copper with a face-centered cubic (FCC) structure have an average size of 10–20 nm. No significant change in the particle size was found when calculated by XRD at the room temperature. However, the over all particle size shown by AFM is much higher as compared with that calculated from XRD. This is because of the fact that the XRD gives the average mean domain size while AFM shows agglomeration of the particles. The XRD and AFM data can be reconciled by the fact that smaller primary particles have a larger surface free energy and would, therefore, tend to agglomerate faster and grow into larger grains. Fig. 2(b) shows the variation of particle size when calculated from the AFM picture and plotted against the percentage volume. It shows that majority of particles came under the range of 20–40 nm due to agglomeration of particles.

2.3. Transmission electron microscopy (TEM) examination

The copper nanofluid was prepared by dispersing copper nanoparticles into water as a base fluid. The reason for using copper nanofluid for the boiling heat transfer studies is the fact that the nanofluids have superior heat transfer characteristics, stability and uniformity. The nanoparticles suspended in the base fluid are exclusive of any noticeable chemical change of the base fluid i.e. water. Further, the physical properties of copper nanofluid can also be determined by using analytical methods. In order to ensure a stable and uniform suspension of nanoparticles in base fluid, the dispersed solution was vibrated in an ultrasonic bath for about 10 h. During this preparation, the nanofluid solution temperature increased from room temperature to nearly 40 °C. Three different mass concentrations of copper nanofluids were prepared for the experiments by controlling the amounts of the particles in base fluids i.e. water and water with 9.0% SDS anionic surfactant. A high resolution transmission electron microscopy (TEM) was used to analyze the size and morphology of the nanoparticles. Fig. 3(a) and (b) shows the copper nanoparticles dispersed in the base fluid of water and its diffraction pattern, respectively. It was approximated that the average size of these very ultra fine particles was 10 nm and these nanoparticles were dispersed in water evenly even after 10 h of ultrasonic vibration. Some of the particles agglomerated and formed cluster due to their inter-molecular attractive force and the average size of the agglomeration was found to be less than 20 nm. Also from the diffraction pattern the structure of the particles was found as polycrystalline.

2.4. Physical properties of nanofluid

In general, the properties of nanofluids depend upon the physical properties of nanoparticles, and the involvement of surface molecules in heat transfer process, which depends upon the size and shape of the particles themselves. The shape and size of particles also affected the agglomeration of the particles. It is to be noted that the flow phenomenon of a liquid–solid solution depends upon the hydrodynamic force acting on the surface of solid particles. The following conversion formula was used to compute the exact volume of nanoparticles:

$$\Phi_v = \frac{1}{\left(\frac{1-\Phi_m}{\Phi_m}\right)\frac{\rho_p}{\rho_f}+1} \tag{2}$$

From the following equations the density and the heat capacity of nanofluids were driven [5]:

$$\rho = \rho_f(1-\Phi_v) + \rho_p\Phi_v \tag{3}$$

$$\rho C_p = \rho_f C_{pf}(1-\Phi_v) + \rho_p C_{pp}\Phi_v \tag{4}$$

Applying the Hamilton and Crosser model [18] to copper nanoparticles in water, the effective thermal conductivity of the copper–water nanofluid was estimated by the following Eq. (5) by Xuan and Li [5]:

$$\frac{k}{k_f} \approx 1 + n\Phi_v \tag{5}$$

where $n = 3/\psi$, and ψ is the sphericity of particles, defined as the ratio of the surface area of a sphere with a volume equal to that of the particle to the surface area of the particle. The effects of particle volume fraction and shape on the thermal conductivity ratio for a copper–water system have been plotted in Fig. 4. The results clearly show that the thermal conductivity of the fluid–particle system depends on both, particle volume fraction and the sphericity as well. For the sphericity of copper nanoparticles as 0.3, the thermal conductivity of water can be enhanced by a factor of 1.003 at the low nanoparticle weight fraction of 0.25%. This finding demonstrates feasibility of nanofluids, i.e. metallic nanoparticles are capable of increasing the thermal conductivity of conventional heat transfer fluids. The following equation can be used for the prediction of viscosity of nanofluid, Brinkman [19]:

$$\mu = \mu_f(1+1.25\Phi_v) \tag{6}$$

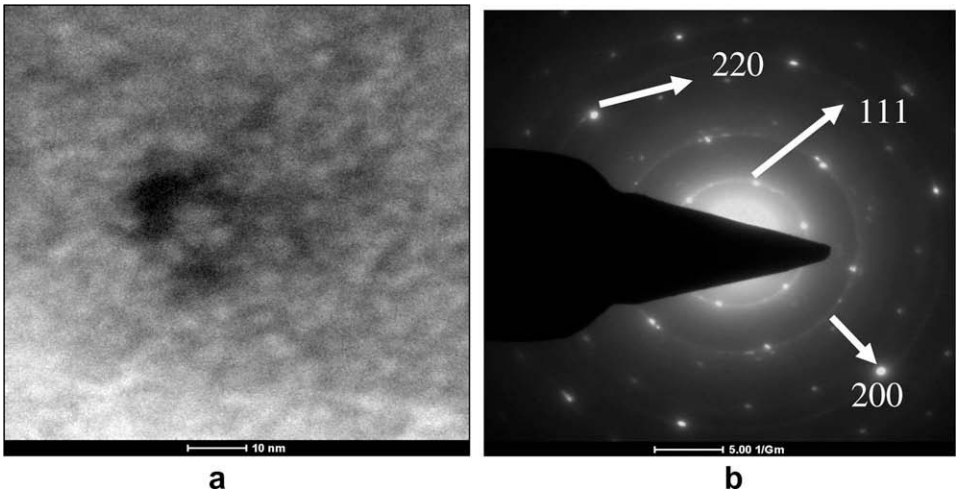

Fig. 3. TEM photographs of water–copper nanofluid.

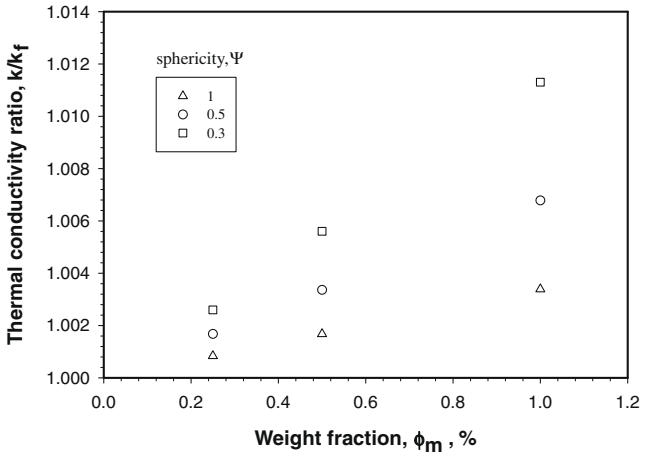

Fig. 4. Variation of thermal conductivity ratio with concentration of nanoparticles.

From the above equations, the major properties of copper nanofluids for various concentrations were determined and are given in Table 1.

3. Experimental set up and procedure for boiling heat transfer studies

Fig. 5(a) shows the schematic diagram of flat plate heater experimental set up. The experimental set up was consisted of emery polished square stainless steel test-heater surface of 30 mm size and 0.44 mm thickness. Two opposite sides of the test-section were brazed with the copper bus bar of 180 mm length and 30 mm × 5 mm cross section. This heater was tightly inserted in to the slot made in the teflon sleeve of diameter of 60 mm through a silicone rubber disc. The other end of copper bars were connected to power supply unit of step down transformer having variable capacity of 10 kVA controlled through a dimmer stat. Five T-type thermocouples were tightly held at different position by the silicone rubber disc and these thermocouples were used to measure the bottom surface temperature of the stainless steel test-section. The thermocouple leads and voltage leads were taken out through five capillary holes made in the teflon sleeve and these leads were connected with data acquisition system. The contact of the thermocouple beads with test-section was ensured by checking the connectivity between them using a multimeter. Fig. 5(b) shows the photographic views of flat plate heater assembly.

This heater assembly was further inserted in the bottom side of the borosilicate glass vessel of inner diameter 60 mm and thickness 4 mm. The vessel has the provision with inlet, drainage, cleaning hole, one vertical reflux glass condenser and thermocouple to measure the bulk temperature of the test-fluid. The vessel arrangement was mounted to the immovable base using mild steel rods of 6 mm diameter, connecting the base and the pressure plate fixed above the vessel using the silicone rubber for leak proof. Finally the experimental set up was checked for any leakage.

Prior to data acquisition, the vessel and test-section were thoroughly cleaned with soap water, distilled water, and finally with acetone to remove any deposition and dirt. After cleaning the test-section was filled with distilled water and was thermally stabilized by heating for 12 h at a heat flux of 500 kW/m^2. Subsequently the test-section was allowed to cool down for another 12 h. In the beginning of data acquisition, the test-fluid was maintained at saturation temperature by given lowest heat flux of 50 kW/m^2 and the generated steam was allowed to pass through the crack valve (3) of condenser to remove any dissolved gases in the test-fluid and in the test-vessel. Then cooling water circulation to the reflux condenser was started simultaneously, so that, any vapor generated by boiling of water was condensed and drained back to the liquid pool through the gravity. The heat flux of the test heater was then increased in steps from 50 kW/m^2 to just before the burn out level and the data were acquired at each step. The entire tests were performed under atmospheric pressure. After the experiments, the distilled water was replaced by water–copper nanofluids of the copper concentrations of 0.25%, 0.5% and 1.0% by weight and finally water–copper nanofluid with 9.0% surfactant of same concentration of copper particles in the mixture. The data were again acquired for the heat flux starting from 50 kW/m^2 to just before the burn out level. After each test conducted, the vessel and heater surfaces were cleaned with a water jet.

Table 1
Major properties of nanofluids.

Copper nanofluid	1	2	3
Φ_m (%)	0.2500	0.5000	1.0000
Φ_v (%)	0.0280	0.0560	0.1130
ρ/ρ_{fo}	1.0020	1.0040	1.0090
C_p/C_{po}	0.9980	0.9960	0.9830
k/k_o	1.0026	1.0056	1.0113
μ/μ_o	1.0007	1.0014	1.0028

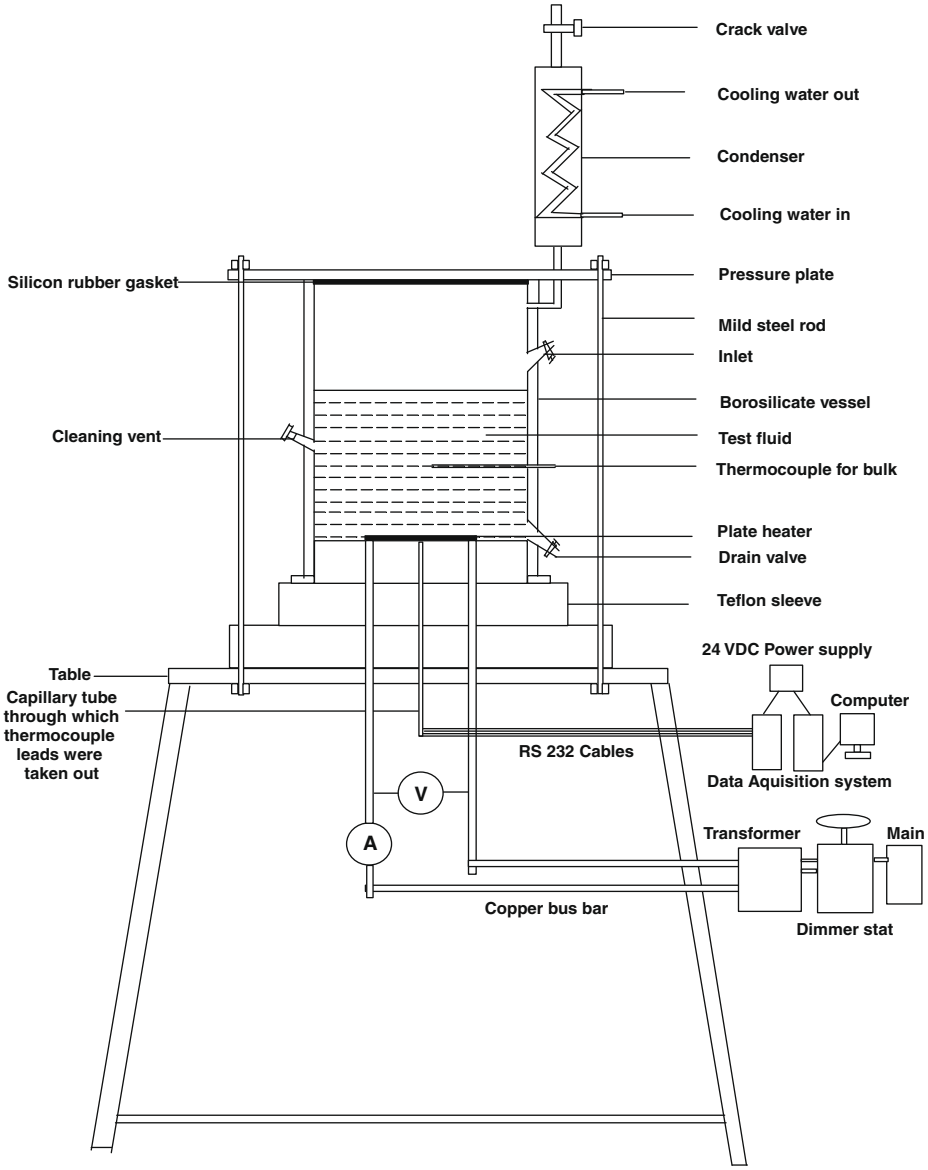

Fig. 5a. Pool boiling experimental set up.

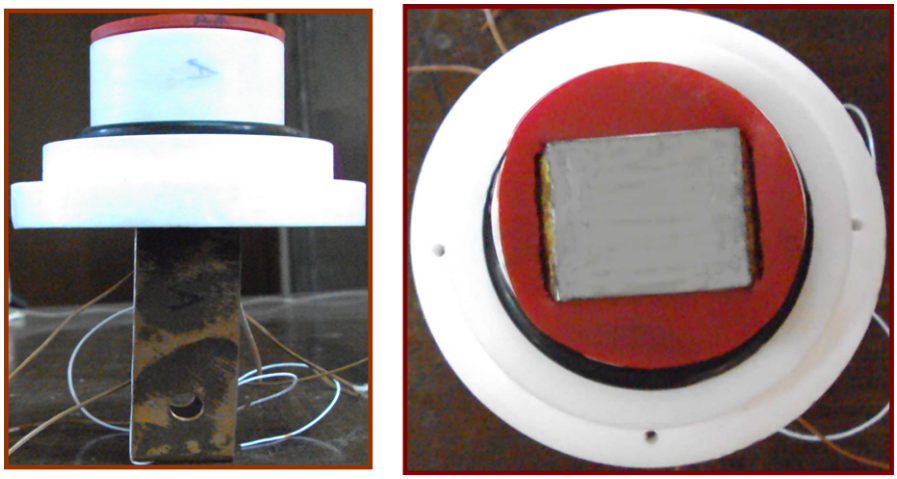

Fig. 5b. Photographic views of heater arrangement.

The wall temperature of plate heater test-section was determined by the following Eq. (7):

$$T_w = \frac{\dot{q}_g}{2k_w}\delta^2 + T_b \tag{7}$$

where T_b is the average bottom surface temperature of test heater determined from the following Eq. (8):

$$T_b = \frac{T_1 + T_2 + T_3 + T_4 + T_5}{5} \tag{8}$$

where T_1, T_2, T_3, T_4, and T_5 are the bottom surface temperature of the test heater located at different places. The average heat transfer coefficient evaluated from the following Eq. (9):

$$h = \frac{q}{T_w - T_{sat}} \tag{9}$$

Although all precautions were taken to minimize the errors in experimentation, yet some errors were likely to creep. The error in measurement depends upon the accuracy of the measuring instruments. An uncertainty analysis of the experimental results has also been carried out. The accuracy in the measurement of temperature, voltage and current was 0.1 °C, 0.1 V and 1.0 A, respectively. The highest experimental uncertainty in heat transfer coefficient was less than 10%.

4. Results and discussion

The data obtained from the boiling of distilled water over a flat plate test heater, have been analyzed in order to check the integrity of the experimental set up. These data shall also be used as reference data to assess the pool boiling characteristics of nanofluids. The heat transfer coefficient for the pool boiling of water have been compared with that predicted by Cornwell–Houston correlation [7] given by the following Eqs. (10) and (11):

$$Nu = 9.7P_c^{0.5}F_pRe^{0.67}Pr^{0.4} \tag{10}$$

$$F_p = 1.8P_r^{0.17} + 4P_r^{1.2} + 10P_r^{10} \tag{11}$$

Fig. 6 shows the comparison of experimental data with Cornwell–Houston correlation [7] taking heat flux, q, as abscissa and heat transfer coefficient, h, as ordinate for the pool boiling of water over the flat surface. The experimental data for the boiling of water are found to be in good agreement with those predicted by Cornwell–Houston [7] correlation. At low heat flux of 200 kW/m^2, the Cornwell–Houston correlation under predicts the experimental data by 30%. As the heat flux increases the predictions from correlation are converge to the experimental values. The results show that the test surface has better heat transfer performance in association with the more bubble nucleation and higher bubble generation frequency [20]. Therefore at higher heat flux the heat transfer curve for experimental data converges towards the predicted values due to high bubble dynamic.

The boiling heat transfer of nanofluid is expected to be higher than that of water due to the fact that the thermal conductivity of the nanofluid is more than that of water. In fact, the properties and behavior of a nanofluid depend upon a number of parameters including the properties of the base liquid and the dispersed phases, particle concentration, particle size and morphology, as well as the presence of dispersants or surfactants [11,12]. Fig. 7(a) shows that for a given wall superheat of test-section the boiling heat transfer of nanofluids is lower than that for pure water as revealed by the shift of boiling curve for nanofluids to the right side of the boiling of pure water. A possible reason for this shift may be the filling up of tube surface cavities by nanoparticles and, thus, reducing the number of nucleation sites on the test-section. Also, it is noticed in Fig. 7(a) that the boiling curve shifts towards right as the concentration on nanoparticles increases in the base fluid i.e. water. This indicates that the boiling heat transfer decreases with an increase of nanoparticles concentration, due to alteration in the microstructure and topography of the test-section by the deposition of nanoparticles. Although at a given wall superheat the heat flux for the nanofluid is lower, yet the critical heat

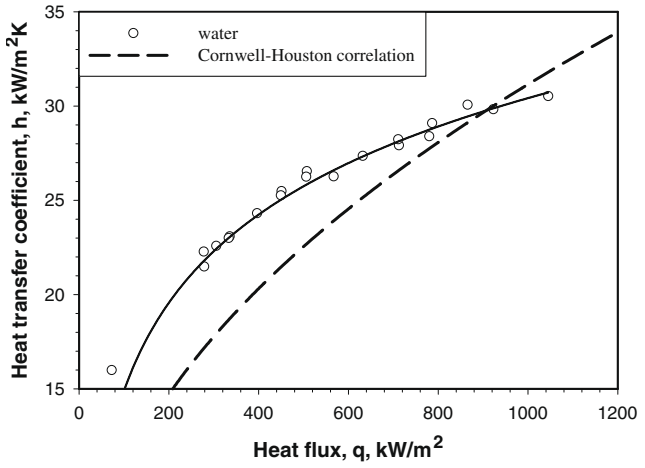

Fig. 6. Variation of experimental data with Cornwell–Houston correlation (Fig. 8). Variation of heat flux with wall superheat.

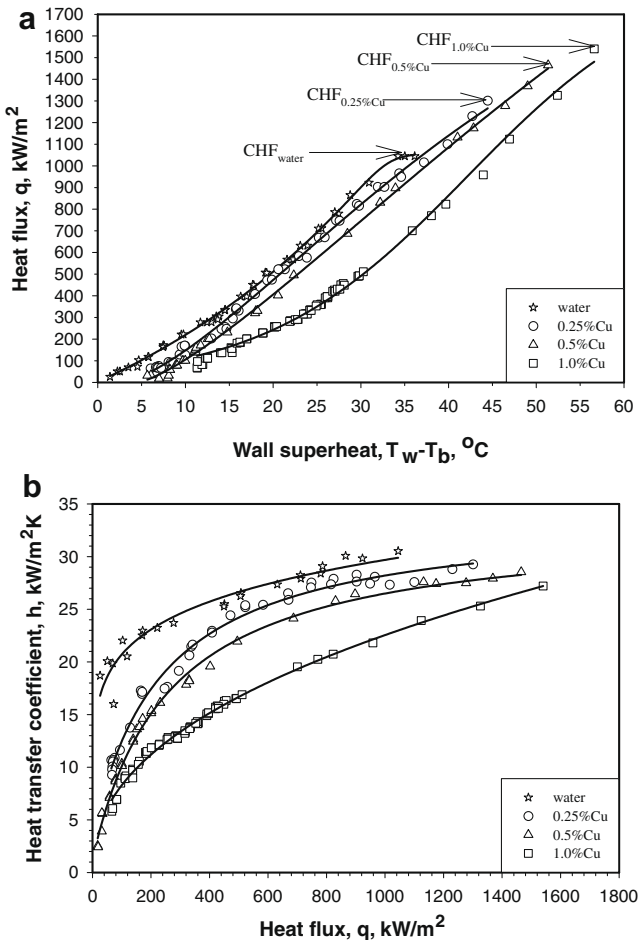

Fig. 7. Comparison of boiling curves of copper–water nanofluids with water (a) $\Delta TVsq$ and (b) $qVsh$.

Table 2
Percentage variation of CHF values of nanofluids with water.

S. No	Test-fluid	CHF MW/m^2	% Increased
1	Water	1.044	–
2	0.25 wt% Cu – water nanofluid	1.305	25
3	0.5 wt% Cu – water nanofluid	1.465	40
4	1 wt% Cu – water nanofluid	1.540	48
			% Decreased
5	Water with surfactant	0.193	82
6	0.25 wt% Cu + surfactant – water nanofluid	0.264	75
7	0.5 wt% Cu + surfactant – water nanofluid	0.335	68
8	1 wt% Cu + surfactant – water nanofluid	0.398	62

flux, CHF, is found to be higher for nanofluids. The CHF of nanofluids for different concentrations of copper are given in Table 2.

Fig. 7(b) has been drawn for copper–water nanofluid, taking heat flux, q, as abscissa and boiling heat transfer coefficient, h, as ordinate. It is found in Fig. 7(b) that for a given heat flux the heat transfer coefficient reduces with increase in the concentration of nanoparticles. This is due to the fact that during the pool boiling of pure water, at low heat flux, only large size cavities are activated. When the heat fluxes increases, the small sized cavities are also activated. But for nanofluid, these cavities were filled with nanoparticles, thus reduced the number of active nucleation sites and hence, reduced the heat transfer coefficient. The boiling phenomenon occurs in the three distinct regimes, viz. nucleate pool boiling, discrete bubble regime, and coalesced bubble regime. With the onset of nucleate boiling and at heat flux higher than 400 kW/m^2, more nucleation sites are activated on the heater surface. The similar phenomenon is also observed by Bang et al. [15] using Al_2O_3 nanofluid taking water as base fluid. However, they achieved the onset of nucleate boiling at the heat flux of 100 kW/m^2. This may be due to the changed heat transfer characteristics of nanofluid used and surface roughness of the heating surface. The change of surface roughness before and after pool boiling experiments of present investigation was found by using Perthometer and is shown in Table 3.

The critical heat flux (CHF) of nanofluids has been compared with that of pure water by a number of investigators. The critical heat flux enhancement is nearly 73% for stainless steel wire with Al_2O_3, ZrO_2 and SiO_2 nanofluids, Kim et al. [14]. In fact, the enhancement in CHF is due to increase of effective contact area by deposition of nanoparticles over the heating surface. The nanoparticles generate a nano porous layer on the test-section tube surface, thus, reducing the contact angle between the fluid and heater surface [21]. Further more, the existence of sorption layer enhances the trapping of liquid in the nano porous sorption layer and prevents the vapor blankets formation. Therefore, the CHF increases with increasing the sorption layer thickness at the low particle concentration range. After the particle concentration exceeds a certain value, the sorption layer thickness would not increase, and therefore, the CHF shall not increase. Fig. 8 shows the enhancement of critical heat flux with concentration of the nanoparticles in the water. Nanoparticles affect the surface characteristics and, therefore, influence the boiling heat transfer. Adaptation of the heater surface by the nanoparticle surface coating was dependent on the particle concentration of the nanofluids. In the case of nanofluids with the lowest particle concentration of 0.25 wt%, the heating surface displayed only a nominal change. However, as the concentration increased, surface deposition of the nanoparticles thickened and more micro-sized structures were formed on the heating surface. A similar phenomenon was also reported by Kim et al. [14] for their pool boiling CHF experiments of water–TiO_2 nanofluids under atmospheric pressure.

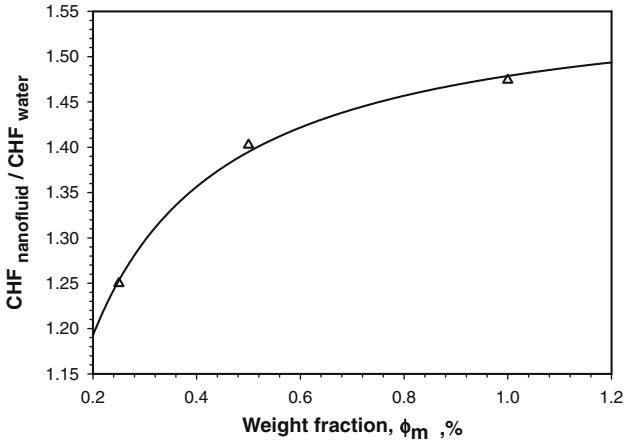

Fig. 8. Increase of critical heat flux with concentration for copper–water nanofluid.

Properties of nanofluids, as given in Table 1, show that the thermal conductivity of water can be enhanced by a factor of 1.003 with a low nanoparticle concentration of 0.25% by weight. The most obvious reason behind the increase of thermal conductivity is the increased surface area due to particle size reduction. However, other factors including Brownian motion, interfacial liquid layering, ballistic transportation of energy carriers within nanoparticles and formation of nanoparticles structure through fractal, clustering and networking, are also important. It is observed that the heated surface, after the boiling tests, is smooth and has a metallic brilliancy and is slightly oxidized. It is also observed that there exists a thin sorption or porous layer on the surface formed by nanoparticles. The sorption layer on the copper surface decreases active nucleation sites and the contact angle, Liu et al. [22]. Less active nucleation sites and the contact angle would delay the inception of boiling and generation of fewer bubbles at a given heat flux. In addition, the sorption layer increases the heat resistance between the metal surface and nanofluid. The surface roughness of heater influences the boiling heat transfer coefficient. The increased surface roughness gives better heat transfer at a given wall superheat [23,24]. Webb et al. [25] also showed the enhancement of boiling heat transfer coefficient of refrigerants by increasing the surface roughness of heaters. This was confirmed through the surface roughness tests conducted before and after the boiling experiments by Perthometer at different places of the test heater and the roughness parameters are tabulated in Table 3. The average surface roughness before boiling experiment was found to be 0.167 μm and it has been reduced to 0.099 μm after the boiling experiments. This is due to nanoparticles deposited over the surface of the test heater and reduces the surface roughness and hence the heat transfer coefficient decreases.

Table 3
Surface roughness parameters of test heater.

S. No	R_q (μm)	R_{max} (μm)	R_a (μm)	R_z (μm)	R_k
Before boiling experiment					
1	0.499	6.66	0.198	1.74	0.23
2	0.570	0.55	0.041	0.33	0.11
3	0.427	2.89	0.246	1.16	0.55
4	0.377	3.22	0.182	0.85	0.10
After boiling experiment					
5	0.155	1.11	0.104	0.70	0.27
6	0.134	1.20	0.093	0.78	0.25
7	0.143	1.15	0.112	0.80	0.37
8	0.116	0.99	0.086	0.64	0.27

Fig. 9 shows a comparison of CHF enhancement obtained in the present case with that of others investigations. From Fig. 9, it is observed that the CHF enhancement is higher in the wire heaters and CHF increases with increase of concentration of the nanoparticles irrespective of nanofluid. The CHF enhancement trend obtained by Kim et al. [13,14] using wire heater is similar to trend obtained by present results. The modification of liquid properties is marginal when compared with the data scattering in Fig. 9, however, the modification of heating surface due to the interaction of nanoparticles become important under high heat flux conditions. This has been suggested by a number of researchers as possible mechanisms for the observed CHF enhancement [9,14]. Such effects can be classified as the roughness, porous effect, improved wettability effect or modified nucleate sites effect.

In the case of water–copper with surfactant nanofluids, Xuan and Li [5] found that the addition of sodium lauryl sulphate (SDS) anionic surfactant, 9.0% by weight, in water-nanoparticles prevent the agglomeration of the particles and gives stable nanofluids for a longer time. In the present investigation also, no settlement has been found for the nanofluids with 9.0% surfactant, even 36 h after the process of ultra sonic vibration. In fact, the surfactant behaves like an interfacial shell between the nanoparticles and base fluids. Surfactant alone modifies the surface tension and wettability of fluids, and influence boiling heat transfer in a significant manner [9,26,27]. Fig. 10(a) and (b) it was observed that the trend of the boiling curves for copper–water with surfactant nanofluids are similar than that of copper–water nanofluids. And also it was observed that for given low heat flux, the difference in heat transfer coefficient is higher for 0.25%, 0.5% and 1.0% copper–water with surfactant nanofluid with each other and it reduced for high heat flux. This is due to high bubble dynamic at high heat fluxes. Fig. 10(a) shows the CHF of pure water decreased due to the addition of 9.0% surfactant (SDS) by weight in copper–water nanofluids. Compared with pure water CHF, it is found that the CHF of 0.25%, 0.5% and 1.0% of copper nanoparticle by weight in copper–water–surfactant nanofluids to be reduced by 75%, 68%, and 62%, respectively. But compared with the CHF of water–surfactant fluid, the

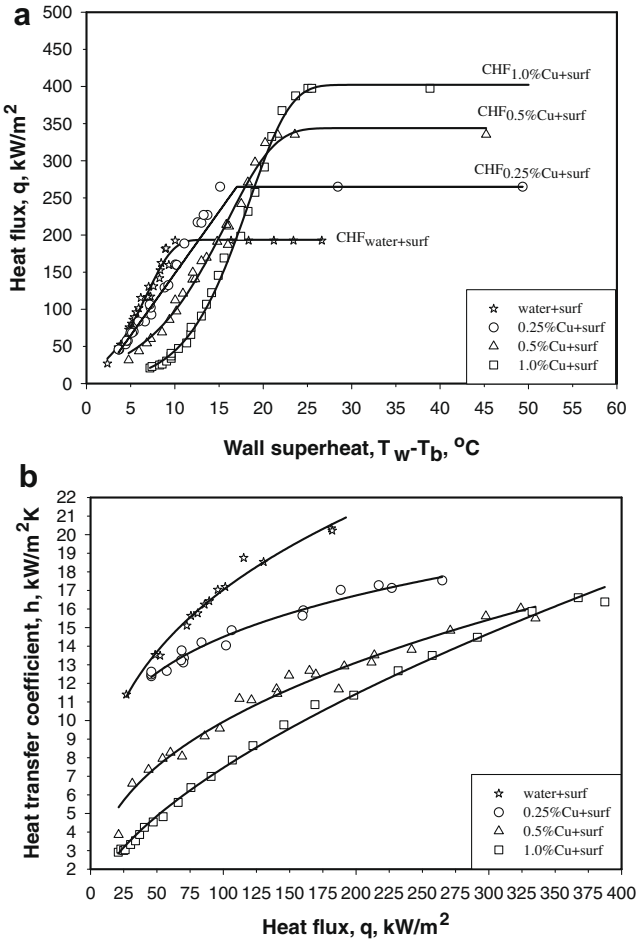

Fig. 10. Boiling curves of copper–water nanofluids with surfactant (a) $\Delta TVsq$ and (b) $qVsh$.

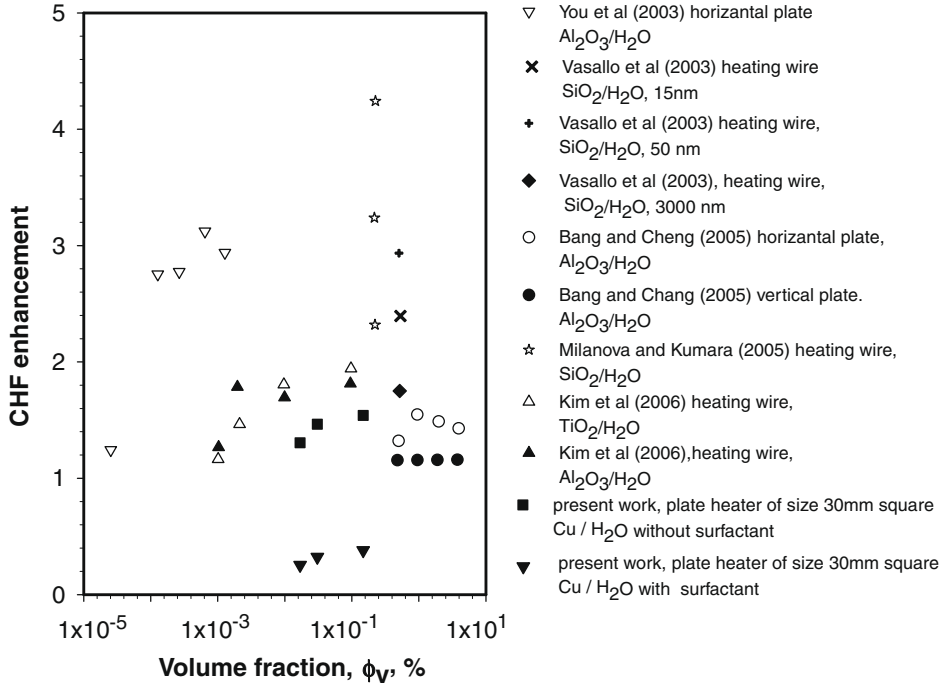

Fig. 9. Comparison of CHF enhancement with other researchers.

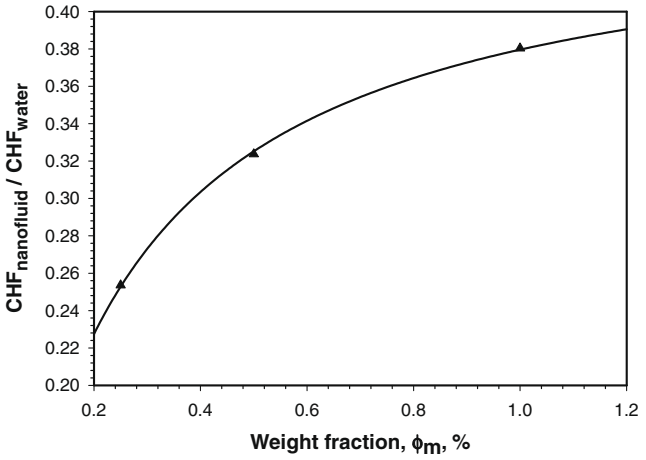

Fig. 11. Critical heat flux with increase of nanoparticles concentration in copper–water nanofluid with 9.0% surfactant.

CHF values of 0.25%, 0.5% and 1.0% of copper nanoparticles in copper–water–surfactant nanofluids are increased by 37%, 74% and 106%, respectively, as shown in Table 2. Fig. 10(b) depicts that the heat transfer coefficient is decreasing when the concentration of nanoparticles increasing for the same heat flux. Furthermore, in the present investigation, during the boiling experiment, it was found that the addition of surfactant increases the bubble dynamic, an early incipience, followed by a rapid departure of smaller-sized and regularly shaped bubbles from the heater surface. Which intern increase the number of active nucleation sites. This is due to the fact that surfactant decreases the dynamic surface tension, and increases the wettability of the heater surface [28]. The critical heat flux obtained in the surfactant nanofluids are given in Table 2. Fig. 11 shows the critical heat flux with increase of concentration of nanoparticles in copper–water nanofluid with 9.0% surfactant. The CHF reduces drastically with the addition of 9.0% surfactant in copper nanofluids. However, with the increase in the concentration of nanoparticles the CHF increases and it attains the highest value at 1.0% concentration of copper nanoparticles, which is only 38% of that for pure water. This is due to the fact that early departure of bubbles growing in the water–surfactant nanofluids increases the wettability of the surface and dynamic surface tension decreases as compared with pure water [28].

5. Conclusions

1. The critical heat flux (CHF) of nanofluids when boiled over a stainless steel flat plate test-section increases with the concentration of copper nanoparticles in the base fluid increases. The highest enhancement when compared to pure water has been found to be 48% and 106% with water and water with 9.0% by weight of surfactant, respectively, when dispersed with 1.0% by weight of copper nanoparticles.
2. Copper nanoparticles cause a decrease in pool boiling heat transfer coefficient for water as base fluid. The heat transfer coefficient decreases as the concentration of nanoparticle increases for both copper–water and copper–water with surfactant nanofluids. The CHF of pure water was decreased by 75%, 68%, and 62% for 0.25%, 0.5% and 1.0% of copper nanoparticle dispersed in water with surfactant nanofluids, respectively, which is purely due to the reduction in surface tension of water by surfactant and high bubble dynamic.
3. The CHF enhancement of nanofluids was closely related to the surface microstructure and enhanced topography resulting from the deposition of nanoparticles on the tube surface. The average surface roughness was reduced from 0.167 to 0.099 μm after the boiling experiments.

References

[1] W.M. Rohsenow, A method of correlating heat transfer data for surface boiling of liquids, Trans. ASME J. Heat Transfer 74 (1952) 969–976.
[2] K. Cornwell, S.D. Houston, Nucleate pool boiling on horizontal tubes: a convection-based correlation, Int. J. Heat Mass Transfer 37 (Suppl. 1) (1994) 303–309.
[3] I.L. Pioro, Experimental evaluation of constants for the Rohsenow pool boiling correlation, Int. J. Heat Mass Transfer 42 (1992) 2003–2013.
[4] Choi Stephen, Nano Fluid Technology: Current Status and Future Research, The Second Korean-American Scientists and Engineers Association Research Trend Study, Vienna, 1998.
[5] Y. Xuan, Q. Li, Heat transfer enhancement of nano fluids, Int. J. Heat Fluid Flow 21 (2000) 58–64.
[6] Y. Xuan, W. Roetzel, Conceptions for heat correlation of nanofluids, Int. J. Heat Mass Transfer 43 (2000) 3701–3707.
[7] S. Lee, U.S. Choi, S. Li, J.A. Eastman, Measuring thermal conductivity of fluids containing oxide nanoparticles, ASME J. Heat Transfer 121 (1999) 280–289.
[8] J.A. Eastman, U.S. Choi, S. Li, W. Yu, L.J. Thompson, Anomalously increased effective thermal conductivities of ethylene glycol-based nanofluids containing copper nano-particles, Appl. Phys. Lett. 78 (2001) 718–720.
[9] P. Vassallo, R. Kumar, S. D'Amico, Pool boiling heat transfer experiments in silica–water nano fluids, Int. J. Heat Mass Transfer 47 (2004) 407–411.
[10] S.M. You, J.H. Kim, K.H. Kim, Effect of nanoparticles on critical heat flux of water in pool boiling heat transfer, Appl. Phys. Lett. 83 (2003) 3374–3376.
[11] S.K. Das, N. Putra, W. Roetzel, Pool boiling characteristics of nanofluids, Int. J. Heat Mass Transfer 46 (2003) 851–862.
[12] S.K. Das, N. Putra, P. Thiesen, W. Roetzel, Temperature dependence of thermal conductivity enhancement for nanofluids, Trans. ASME J. Heat Transfer 125 (2003) 567–575.
[13] Hyungdae Kim, Jeongbae Kim, Moo Hwan Kim, Effect of nanoparticles on CHF enhancement in pool boiling of nanofluids, Int. J. Heat Mass Transfer 49 (2006) 5070–5074.
[14] H. Kim, J. Kim, M. Kim, Experimental study on CHF characteristics of water–TiO_2 nano fluids, Nucl. Eng. Technol. 38 (1) (2006) 61–69.
[15] I.C. Bang, S.H. Chang, Boiling heat transfer performance and phenomena of Al_2O_3–water nanofluids from a plain surface in a pool, Int. J. Heat Mass Transfer 48 (2005) 2407–2419.
[16] Dongsheng Wen, Yulong Ding, Experimental investigation into the pool boiling heat transfer of aqueous based γ-alumina nano fluids, J. Nanopart. Res. 7 (2005) 265–274.
[17] B.D. Cullity, S.R. Stock, Text Book of Elements of X-ray Diffraction. third ed., Prentice-Hall Publiser, pp. 170 (Chapter 5).
[18] R.L. Hamilton, O.K. Crosser, Thermal conductivity of heterogeneous two-component systems, Ind. Eng. Chem. Fundam. 1 (1962) 187–191.
[19] H.C. Brinkman, The viscosity of concentrated suspensions and solutions, J. Chem. Phys. 20 (1952) 571–581.
[20] J.Y. Tsay, Y.Y. Yan, T.F. Lin, Enhancement of pool boiling heat transfer in a horizontal water layer through surface roughness and screen coverage, Heat Mass Transfer 32 (1996) 17–26.
[21] S.J. Kim, I.C. Bang, J. Buongiorno, L.W. Hu, Surface wettability change during pool boiling of nanofluids and its effect on critical heat flux, Int. J. Heat Mass Transfer 50 (2007) 4105–4116.
[22] Z.H. Liu, Y.H. Qiu, Boiling heat transfer characteristics of nano fluids jet impingement on a plate surface, J. Heat Mass Transfer 43 (2007) 699–706.
[23] M.G. Kang, Effect of surface roughness on pool boiling heat transfer, Int. J. Heat Mass Transfer 43 (2000) 4073–4085.
[24] Z.H. Liu, Y.H. Qiu, Enhanced boiling heat transfer in restricted spaces of a compact tube bundle with enhanced tubes, Appl. Therm. Eng. 22 (2002) 1931–1941;
Z.H. Liu, Y.H. Qiu, Enhanced boiling heat transfer in restricted spaces of a compact tube bundle with enhanced tubes, Appl. Therm. Eng. (2003) 567–574.
[25] R.L. Webb, C. Pais, Nucleate pool boiling data for five refrigerants on plain, integral-fin and enhanced tube geometries, Int. J. Heat Mass Transfer 35 (1992) 1893–1904.
[26] G. Hetsroni, M. Gurevich, A. Mosyak, R. Rozenblit, Z. Segal, Boiling enhancement with environmentally acceptable surfactants, Int. J. Heat Fluid Flow 25 (2004) 841–848.
[27] D.S. Wen, Y.L. Ding, R. Williams, Pool-boiling heat transfer of aqueous based TiO_2 nanofluids, J. Enhanced Heat Transfer 13 (2006) 231–244.
[28] C.H. Wang, V.K. Dhir, Effect of surface wettability on active nucleation site density during pool boiling of water on a vertical surface, J. Heat Transfer 115 (1993) 659–669.